



## Article

# Benzalkonium Chloride, Even at Low Concentrations, Deteriorates Intracellular Metabolic Capacity in Human Conjunctival Fibroblasts

Yuri Tsugeno <sup>1</sup>, Tatsuya Sato <sup>2,3</sup>, Megumi Watanabe <sup>1</sup>, Masato Furuhashi <sup>2</sup>, Araya Umetsu <sup>1</sup>, Yosuke Ida <sup>1</sup>, Fumihito Hikage <sup>1</sup> and Hiroshi Ohguro <sup>1,\*</sup>

<sup>1</sup> Departments of Ophthalmology, School of Medicine, Sapporo Medical University, Sapporo 060-8556, Japan

<sup>2</sup> Departments of Cardiovascular, Renal and Metabolic Medicine, Sapporo Medical University, Sapporo 060-8556, Japan

<sup>3</sup> Departments of Cellular Physiology and Signal Transduction, Sapporo Medical University, Sapporo 060-8556, Japan

\* Correspondence: ooguro@sapmed.ac.jp; Tel.: +81-611-2111

**Abstract:** The objective of this study was to clarify the effects of benzalkonium chloride (BAC) on two-dimensional (2D) and three-dimensional (3D) cultures of human conjunctival fibroblast (HconF) cells, which are in vitro models replicating the epithelial barrier and the stromal supportive functions of the human conjunctiva. The cultured HconF cells were subjected to the following analyses in the absence and presence of 10<sup>-5</sup>% or 10<sup>-4</sup>% concentrations of BAC; (1) the barrier function of the 2D HconF monolayers, as determined by trans-endothelial electrical resistance (TEER) and FITC dextran permeability, (2) real-time metabolic analysis using an extracellular Seahorse flux analyzer, (3) the size and stiffness of 3D HconF spheroids, and (4) the mRNA expression of genes that encode for extracellular matrix (ECM) molecules including collagen (COL)1, 4 and 6, and fibronectin (FN),  $\alpha$ -smooth muscle actin ( $\alpha$ -SMA), ER stress related genes including the X-box binding protein-1 (XBP1), the spliced XBP1 (sXBP1) glucose regulator protein (GRP)78, GRP94, and the CCAAT/enhancer-binding protein homologous protein (CHOP), hypoxia inducible factor 1 $\alpha$  (HIF1 $\alpha$ ), and Peroxisome proliferator-activated receptor gamma coactivator 1 $\alpha$  (PGC1 $\alpha$ ). In the presence of BAC, even at low concentrations at 10<sup>-5</sup>% or 10<sup>-4</sup>%, the maximal respiratory capacity, mitochondrial respiratory reserve, and glycolytic reserve of HconF cells were significantly decreased, although the barrier functions of 2D HconF monolayers, the physical properties of the 3D HconF spheroids, and the mRNA expression of the corresponding genes were not affected. The findings reported herein highlight the fact that BAC, even such low concentrations, may induce unfavorable adverse effects on the cellular metabolic capacity of the human conjunctiva.

**Keywords:** 3D spheroid cultures; human conjunctival fibroblast (HconF); benzalkonium chloride (BAC)



**Citation:** Tsugeno, Y.; Sato, T.; Watanabe, M.; Furuhashi, M.; Umetsu, A.; Ida, Y.; Hikage, F.; Ohguro, H. Benzalkonium Chloride, Even at Low Concentrations, Deteriorates Intracellular Metabolic Capacity in Human Conjunctival Fibroblasts. *Biomedicines* **2022**, *10*, 2315. <https://doi.org/10.3390/biomedicines10092315>

Academic Editor: Nadezhda S. Kudryasheva

Received: 24 August 2022

Accepted: 14 September 2022

Published: 18 September 2022

**Publisher's Note:** MDPI stays neutral with regard to jurisdictional claims in published maps and institutional affiliations.



**Copyright:** © 2022 by the authors. Licensee MDPI, Basel, Switzerland. This article is an open access article distributed under the terms and conditions of the Creative Commons Attribution (CC BY) license (<https://creativecommons.org/licenses/by/4.0/>).

## 1. Introduction

It is well known that medical instillation therapy in the treatment of chronic ocular diseases including glaucoma, dry eye, and others can cause ocular surface adverse effects (OSAE) that can affect the eyelids, conjunctiva, and/or corneal epithelium [1–4], with the following symptoms often being associated with these conditions; redness, irritation, burning, fatigue, deteriorating visual acuity, infections, and others. As a possible causative factor, it has been suggested that for OSAE, toxicity by benzalkonium chloride (BAC), which is most commonly used in concentrations of 4–2 × 10<sup>-2</sup>% as a preservative in topical ophthalmic formulations [2–6], toward ocular tissue cells is the likely cause. The threshold concentration for inducing such toxic effects has been estimated to be approximately ~5 × 10<sup>-3</sup>% based upon several in vitro and in vivo studies showing that BAC exposure

induced (1) a reduced survival of corneal cells [7–12], conjunctival cells [7,8,13,14], trabecular meshwork (TM) cells [15,16], and ciliary epithelial cells [9,13,15,17], loss of conjunctival goblet cells [13,14], (2) delayed corneal epithelial wound healing [18], (3) the induction of lymphocyte infiltration into conjunctival tissue [13,17], and (4) an increase in the levels of inflammatory cytokines in ocular tissues [9,10,12]. Alternatively, several clinical studies have reported that these BAC-induced adverse effects may partially be reversible upon withdrawal of the exposure to BAC [19–24].

However, in contrast, another previous study indicated that a short time exposure (30 min) to much lower concentrations of BAC ranging from  $5 \times 10^{-5}\%$  ~ or  $10^{-3}\%$  toward immortalized human corneal epithelial cells (HCEs) caused DNA double-strand breaks (DSBs) and these breaks were concentration-dependent [25]. This information rationally suggests that BAC-induced risk may be evoked, even when much lower concentrations ( $5 \times 10^{-5}\%$  ~ or  $10^{-3}\%$ ) of BAC are used as compared with the above estimated threshold levels. Therefore, to study the cytotoxic effects of BAC at much lower concentrations ( $10^{-5}\%$  and  $10^{-4}\%$ ) toward conjunctival tissues, we employed recently established in vitro models for the epithelial barrier and the stromal supportive functions of the human conjunctiva using two-dimension (2D) and three-dimension (3D) spheroid cultures of the human conjunctival fibroblasts (HconF) cells [26], and the following analyses were carried out: (1) barrier functions of 2D cultured HconF monolayers by trans-endothelial electron resistance (TEER) and FITC dextran permeability measurements, (2) measurements of real-time mitochondrial and glycolytic cellular function, (3) measurements of the size and hardness of the 3D HconF spheroids, and (4) quantitative PCR of major extracellular matrix (ECM) molecules, including collagen (COL)1, 4 and 6, and fibronectin,  $\alpha$ -smooth muscle actin ( $\alpha$ -SMA), ER stress related genes including the X-box binding protein-1 (XBP1), the spliced XBP1 (sXBP1) glucose regulator protein (GRP)78, GRP94, and the CCAAT/enhancer-binding protein homologous protein (CHOP), hypoxia inducible factor 1 $\alpha$  (HIF1 $\alpha$ ), and Peroxisome proliferator-activated receptor gamma coactivator 1 (PGC1 $\alpha$ ).

## 2. Materials and Methods

### 2.1. 2D Cell and 3D Spheroid Cultures of Human Conjunctival Fibroblasts (HconF)

BAC powder (CAS#8001-54-5, Nacalai Tesque, Kyoto, Japan) was dissolved in DMEM (FUJIFILM Wako Pure Chemical Corporation, Osaka, Japan) adjusted to a concentration of 0.2%, and further diluted in 10% FBS (BioWest, Nuaille, France). As a negative control, the same diluent was used. In the presence  $10^{-5}\%$  or  $10^{-4}\%$  BAC, or only diluent, HconF cells (ScienCell Research laboratories, CA U.S.A.) were 2D cultured and further maintained or subjected to 3D spheroid culturing for 6 days using hanging drop culture plates (# HDP1385, Sigma-Aldrich, St Louis, MO, USA), as described in our previous study [26]. Briefly, 2D cultured HconF cells in 150 mm 2D culture dishes at 37 °C in the Fibroblast Medium (FM, Cat. #2301, ScienCell Research laboratories, Carlsbad, CA, USA) [26] were maintained by changing the medium every other day. Alternatively, these 2D cultured HconF cells were washed with phosphate buffered saline (PBS), detached using 0.05% Trypsin/EDTA (FUJIFILM Wako Pure Chemical Corporation, Osaka, Japan), and re-suspended in the Fibroblast Medium supplemented with 0.25% methylcellulose (Methocel®A4M, Sigma-Aldrich, St Louis, MO, USA). Then, approximately 20,000 HconF cells in 28  $\mu$ L of the suspension were subjected to each well of the 3D hanging drop culture plate (# HDP1385, Sigma-Aldrich) (Day 0). Thereafter, on each following day until Day 6, half of the medium (14  $\mu$ L) was exchanged by fresh medium.

### 2.2. Analysis of the Barrier Function of 2D HconF Cell Monolayers by TEER and FITC Dextran Permeability

In the absence and presence of  $10^{-5}\%$  or  $10^{-4}\%$  BAC, HconF cells were 2D cultured using a TEER plate (0.4  $\mu$ m pore size and 12 mm diameter; Corning Transwell, Sigma-Aldrich) at 37 °C in the Fibroblast Medium as above. On Day 6, the TEER values between the 2D HconF monolayer were measured using an electrical resistance system (KANTO

CHEMICAL CO. INC., Tokyo, Japan), and FITC-dextran permeability was estimated by measuring the fluorescence intensity that had permeated through the membrane from the basal compartment to the apical compartment during a period of 60 min as described in our previous study [27].

### 2.3. Seahorse Real-Time Bio-Cellular Metabolic Function Analysis of the 2D HconF Cells

As the bio-cellular function of 2D HconF cells, their oxygen consumption rate (OCR) and the extracellular acidification (ECAR) of  $10^{-5}\%$  or  $10^{-4}\%$  BAC-treated or un-treated 2D HconF cells were evaluated by a Seahorse XFe96 Bioanalyzer (Agilent Technologies, Santa Clara, CA, USA) as described in the previous studies [28,29]. In brief, approximately 20,000 2D cultured HconF cells per well were set in an XFe96 Cell Culture Microplate (Agilent Technologies, #103794-100). The plate was centrifuged at  $1600 \times g$  for 10 min, and the culture medium was replaced with 180  $\mu$ L of assay buffer (Seahorse XF DMEM assay medium with 5.5 mM glucose, 2.0 mM glutamine, 1.0 mM sodium pyruvate (pH 7.4, Agilent Technologies, #103575-100)). Then, the assay plate was incubated in a  $\text{CO}_2$ -free incubator at  $37^\circ\text{C}$  for 1 h prior to the assay. OCR and ECAR were simultaneously measured on a Seahorse XFe96 Bioanalyzer under a 3-min-mixing and 3-min-measuring protocols using the following sequential injection of oligomycin (final concentration: 2.0  $\mu$ M), carbonyl cyanide p-trifluoromethoxyphenylhydrazone (FCCP, final concentration: 5.0  $\mu$ M), rotenone/antimycin A mixture (final concentration: 1.0  $\mu$ M), and 2-deoxyglucose (2-DG, final concentration: 10 mM). Values of OCR and ECAR were normalized to the total protein per well after completion of assay.

### 2.4. Evaluation of the Size and Hardness of HconF Cell 3D Spheroids

The analyses of the physical properties, size, and hardness of the HconF 3D spheroids were performed as reported in our previous studies [30,31]. Briefly, the mean sizes of the 3D spheroids were measured using an inverted microscope (Nikon ECLIPSE TS2; Tokyo, Japan). Alternatively, for the hardness measurement, a single living 3D spheroid was placed on a 3-mm  $\times$  3-mm plate and compressed to achieve a 50% deformation during 20 seconds using a micro-compressor (MicroSquisher, CellScale, Waterloo, ON, Canada). The required force ( $\mu$ N) was measured, and force/displacement ( $\mu$ N/ $\mu$ m) was calculated.

### 2.5. Other Analytical Methods

Total RNA was extracted from the 2D or 3D cultured HconF cells and those were subjected to reverse transcription and real-time PCR as previously reported [32,33] using specific primers and probes (Supplemental Table S1).

As described in a recent report [32,33], all statistical analyses were performed using Graph Pad Prism 8 (GraphPad Software, San Diego, CA, USA). A significant difference at less than 0.05 between experimental groups by ANOVA followed by a Tukey's multiple comparison test was determined as statistically significant.

## 3. Results

Among ocular surfaces, the conjunctiva is well known to be involved in two different biological roles, namely, (1) a biological barrier by conjunctival epithelium [34] and (2) ocular tissue support, repair, and remodeling by conjunctival stroma [35,36]. In the current study, to investigate the effects of low concentrations of BAC at  $10^{-5}\%$  or  $10^{-4}\%$  on these conjunctival functions, under which no significant cytotoxicity was observed (Figure S1), we employed our recently established in vitro model using 2D and 3D cultures of HconF cells [26] which are thought to be related to the epithelial and stromal functions, respectively.

In a previous study we showed that, as the barrier function of the corneal epithelium, TEER values had significantly deteriorated even after a 20 min exposure to  $10^{-3}\%$  of BAC [11]. Furthermore,  $10^{-4}\%$  BAC also caused the significant up-regulation of IL-6 and IL-8 genes of 2D and the Matrigel<sup>®</sup>-assisted 3D spheroids of human trabecular meshwork

(HTM) cells [37], although cytotoxic effects by BAC ( $2 \times 10^{-2}\%$ ) were not detected in the 3D corneal epithelial culture model [38]. However, in our established in vitro 3D spheroid model using HconF cells [26], HTM cells [31,39], human corneal stromal fibroblasts (HCSFs) [40] and human orbital fibroblast (HOFs) [41,42], several drugs including those treated with  $\text{PGF2}\alpha$ , ROCK inhibitors, and others failed to induce cytotoxic effects but their physical properties were greatly modulated. These collective findings suggest that our established measurements of these physical properties of the 3D spheroids should be more sensitive in estimating cellular biological aspects, and therefore, it would be possible to use this methodology to evaluate effects of concentrations of BAC as low as  $10^{-5}\%$  or  $10^{-4}\%$ . Thus, initially, to study such low concentrations of BAC-induced effects on barrier function, TEER and FITC dextran permeability measurements of 2D HconF cell monolayers were conducted. As shown in Figure 1, both measurements were not affected at all by the presence of both  $10^{-5}\%$  and  $10^{-4}\%$  of BAC. Next, to estimate the influences of these low concentrations of BAC toward the tissue supportive functions of conjunctiva, the 3D HconF spheroid model was used. The result indicated that their physical properties, size, and stiffness were also not altered by these concentrations of BAC as similarly to the barrier functions of the 2D monolayer as above (Figure 2).

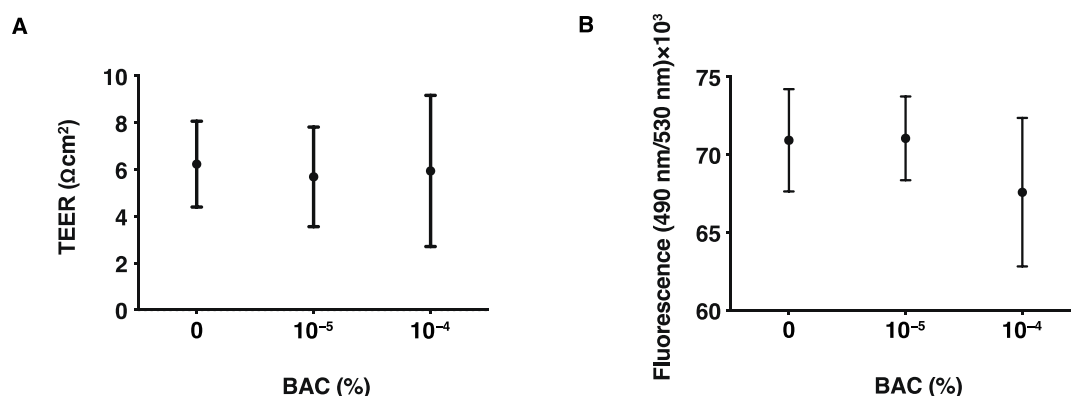


**Figure 1.** Effects of benzalkonium chloride (BAC) on barrier functions of HconF 2D monolayers. Barrier function based on TEER and FITC dextran permeability measurements were made on HconF cell 2D monolayers in the absence or presence of  $10^{-5}\%$  or  $10^{-4}\%$  BAC. Plots of the electric resistance ( $\Omega\text{cm}^2$ ) by TEER and the absorbance of the amounts of permeated fluorescein are shown in (A) and (B), respectively. Experiments were repeated in triplicate ( $n = 5$  each). All data are expressed; the mean  $\pm$  the standard error of the mean (SEM). Statistical significance was evaluated by ANOVA followed by a Tukey's multiple comparison test.

To elucidate additional aspects related to the BAC-induced effects on the cellular physiology of the 2D HconF cells, mitochondria- and glycolysis-related functions were evaluated by a Seahorse real-time bio-cellular analyzer, since previous studies showed that upon BAC exposure, the OCR of rat liver mitochondria was substantially deteriorated [43], and glycolysis in bacteria was greatly modulated [44]. However, mitochondrial maximal respiration, mitochondrial respiratory reserve, and glycolytic reserve in HconF cells were significantly decreased by the presence of BAC, even at low concentrations, suggesting that BAC can adversely affect intracellular metabolic capacity (Figure 3A–D). The energy map visually indicated that metabolic response induced by FCCP-induced stress in HconF cells was impaired even with  $10^{-4}\%$  BAC exposure, while BAC had no effect on baseline metabolism at either  $10^{-5}\%$  and  $10^{-4}\%$  concentrations (Figure 3E). These functional assays suggested that cellular mitochondrial and glycolytic functions were already affected even though the barrier functions by TEER and FITC dextran permeability of the 2D HconF monolayer and physical properties of the 3D HconF spheroid were not influenced in the presence of  $10^{-5}\%$  and  $10^{-4}\%$  BAC.

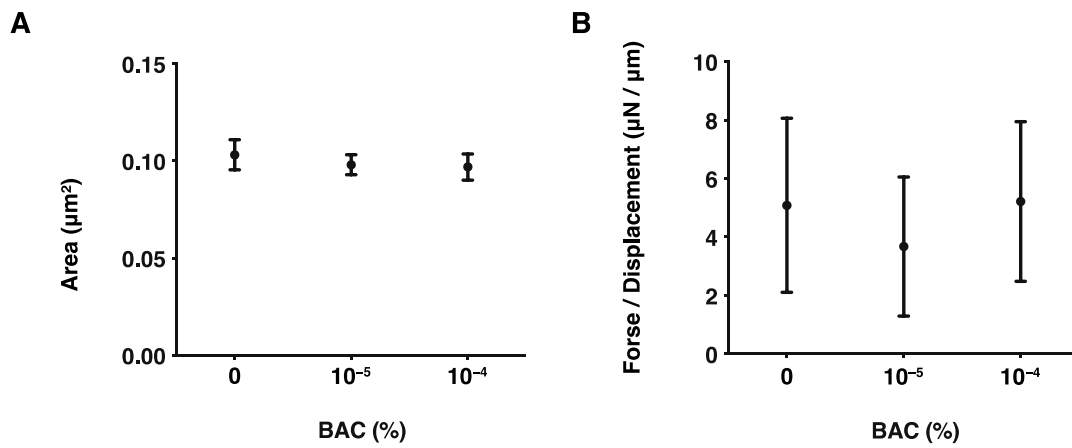


**Figure 2.** Effects of BAC on the sizes and hardness of the HconF 3D spheroids. Analysis of the size and hardness of 3D HconF spheroids in the absence or presence of 10<sup>-5</sup>% or 10<sup>-4</sup>% BAC. The mean sizes (µm) and the force required to compress a single spheroid to the semidiameter (µN/µm) within 20 seconds are plotted in (A) and (B), respectively. Experiments were repeated in triplicate using fresh preparations (n = 16 spheroids each). All data are expressed; the mean ± the standard error of the mean (SEM). Statistical significance was evaluated by ANOVA followed by a Tukey’s multiple comparison test.

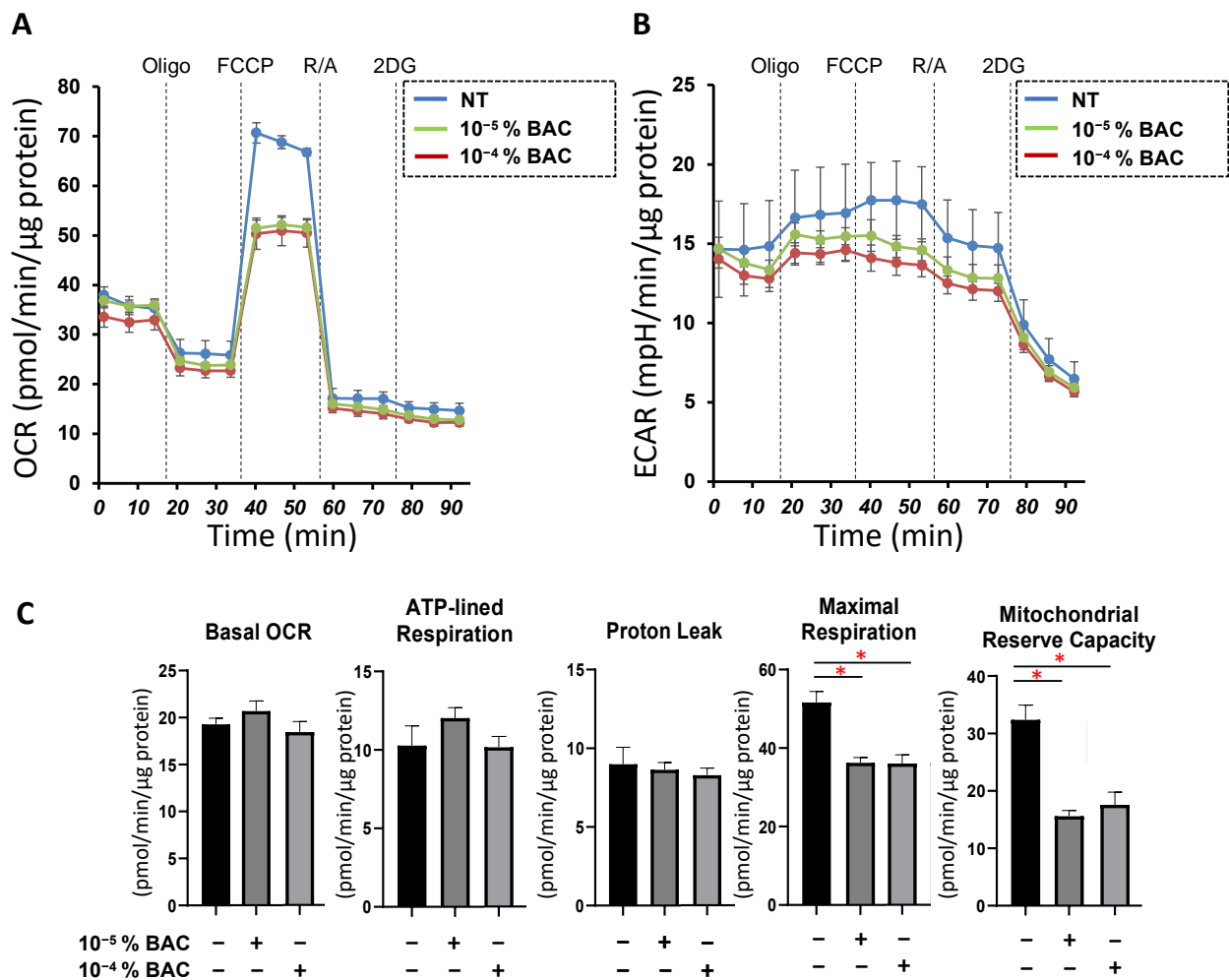


**Figure 3.** Cont.

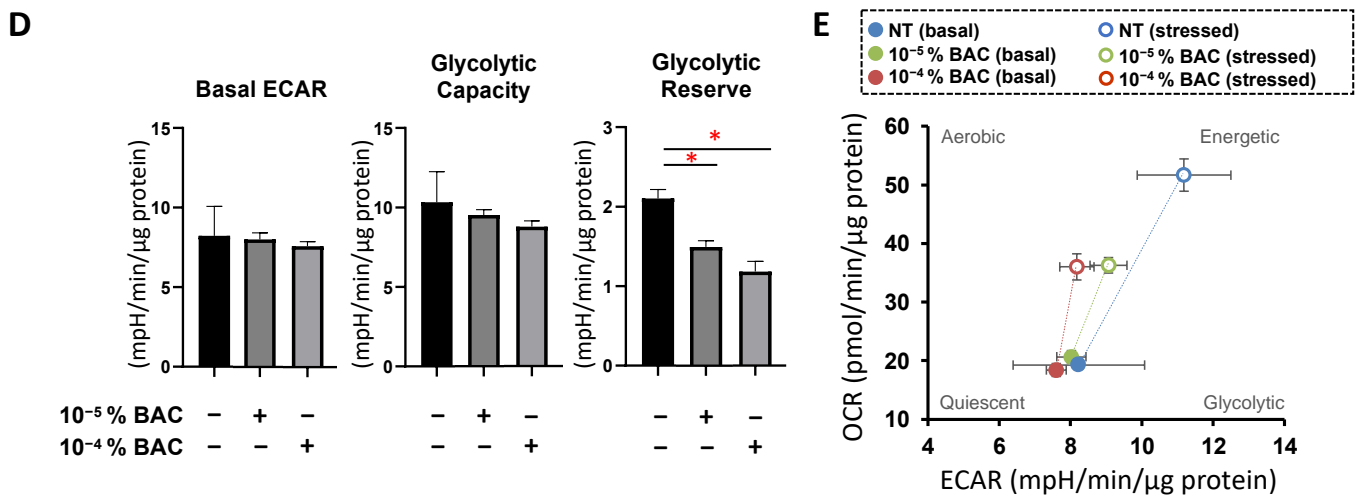


**Figure 3.** Effects of BAC on the mitochondrial and glycolytic functions in HconF 2D cells. A Seahorse real-time metabolic function analysis of HconF cells in the absence (blue dots, NT) or presence of BAC at concentrations of 10<sup>-5</sup>% (green dots) or 10<sup>-4</sup>% (brown dots) BAC. OCR (A) and ECAR (B) were measured at baseline and those with injections of sequential supplementation with a complex V inhibitor, oligomycin (Oligo), a protonophore, Carbonyl cyanide-p-trifluoromethoxyphenylhydrazone (FCCP), complex I/III inhibitors, rotenone/antimycin A (R/A), and a hexokinase inhibitor, 2-deoxyglucose (2DG). (C) Indicates the parameters of mitochondrial function. Basal OCR was calculated as the difference in OCR at the baseline and after the addition of R/A. ATP-linked respiration was calculated as the difference in OCR at the baseline and after the addition of Oligo. Proton leak was calculated as the difference between OCR after the addition of Oligo and OCR after the addition of R/A. Maximal respiration was calculated as the difference between OCR after the addition of FCCP and after the addition of R/A. Mitochondrial reserve capacity was calculated as the difference in OCR at baseline and after the addition of FCCP. (D) Indicates parameters of glycolytic function. Basal ECAR was calculated as the difference in ECAR at baseline and after the addition of 2DG. Glycolytic capacity was calculated as the difference between ECAR after the addition of Oligo and ECAR after the addition of 2DG. Glycolytic reserve was calculated as the difference in ECAR at baseline and after the addition of Oligo. (E) Energy map for cells in the absence or presence of 10<sup>-5</sup>% and 10<sup>-4</sup>% BAC. Experiments were performed using fresh preparations (n = 3). Data are expressed; the mean ± the standard error of the mean (SEM). \* *p* < 0.05; ANOVA followed by a Tukey's multiple comparison test.

To study this issue further, the expressions of several genes including major ECM molecules including COL 1,4 and 6, FN and  $\alpha$ -SMA, ER stress related factors, HIF1 $\alpha$ , and PGC1 $\alpha$  were analyzed by qPCR. As shown in Figures 4–6, mRNA expression of these molecules was not altered by these concentrations of BAC. Taken together with these gene expression analyses, Seahorse real time bio-metabolic measurements related to mitochondrial and glycolysis may be much more sensitive for evaluation of the physiological states of the living cells as compared with gene expressions of several related factors as well as physical analyses. Thus, these collective results suggest that some functional and morphological abnormality may be induced within human conjunctiva, even when such low concentrations of BAC are being used, especially in case with their long-term exposure.

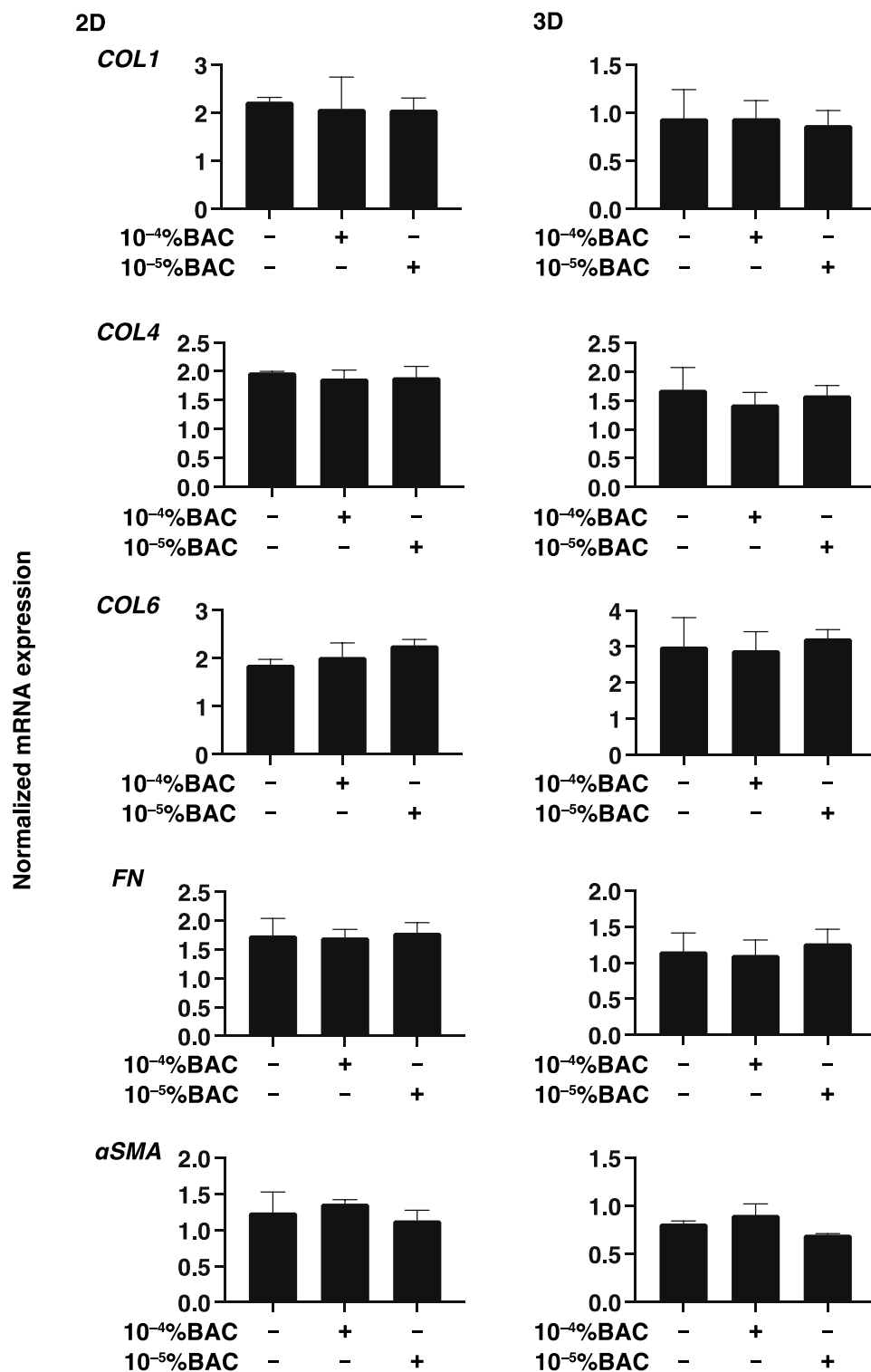


**Figure 4.** Effects of BAC on the gene expression of ECMs of HconF cells. 2D and 3D HconF cells were subjected to qPCR analysis for ECMs including COL1, COL4, COL6, FN, and αSMA in the absence or presence of 10<sup>-5</sup>% or 10<sup>-4</sup>% BAC. Experiments were repeated in triplicate using 3 different confluent 6-well dishes (2D) or 15 freshly prepared 3D HconF spheroids (3D) in each experimental condition. All data are expressed; the mean ± the standard error of the mean (SEM). Statistical significance was evaluated by ANOVA followed by a Tukey's multiple comparison test.

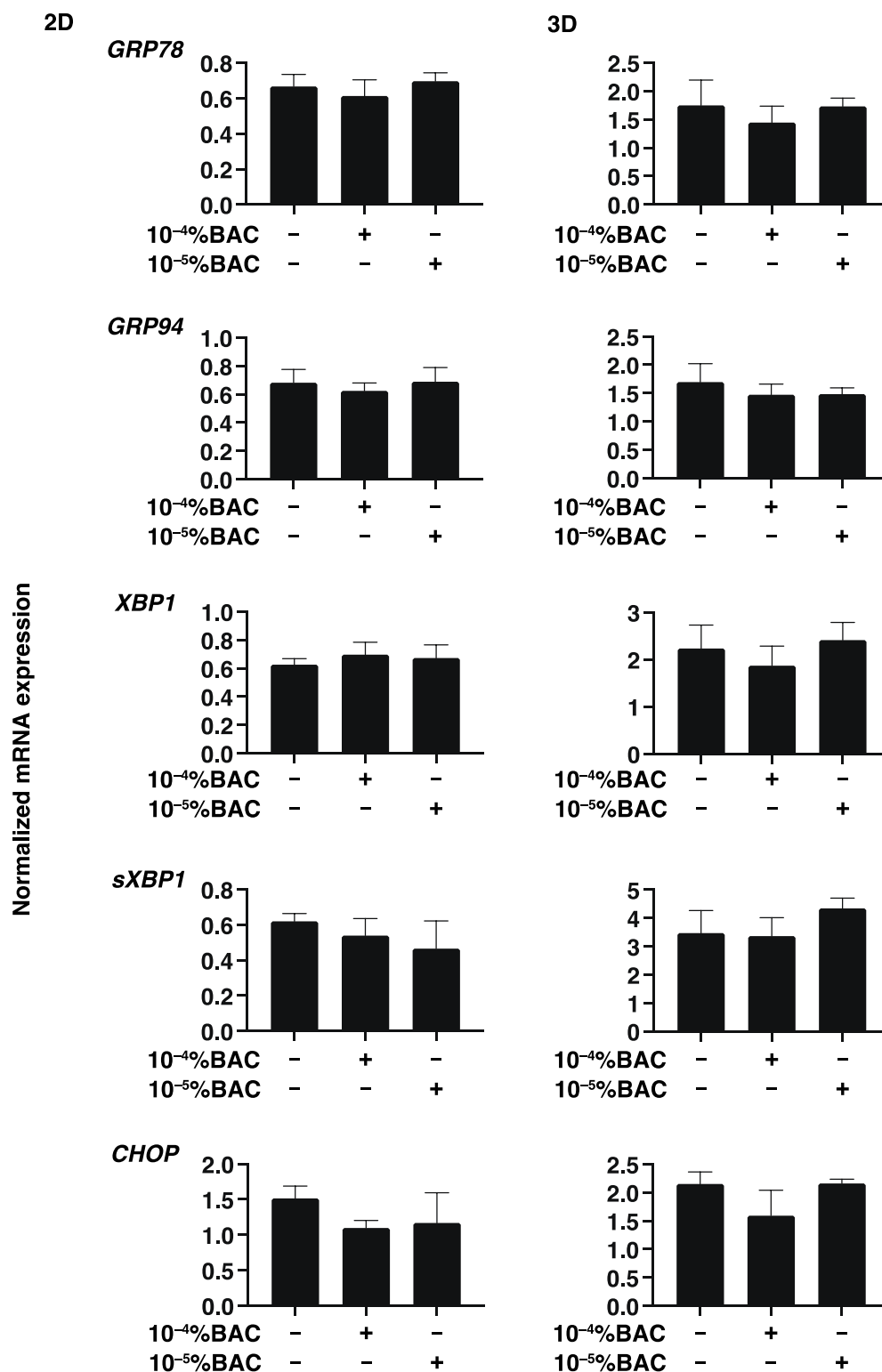


**Figure 5.** Effects of BAC on the gene expression of ER stress related factors of HconF cells. 2D and 3D HconF cells were subjected to qPCR analysis of ER stress-related genes in the absence or presence of  $10^{-5}\%$  or  $10^{-4}\%$  BAC; the glucose regulator protein (GRP)78, GRP94, the X-box binding protein-1 (XBP1), spliced XBP1 (sXBP1), and CCAAT/enhancer-binding protein homologous protein (CHOP). Experiments were repeated in triplicate using 3 different confluent 6-well dishes (2D) or 15 freshly prepared 3D HconF spheroids (3D) in each experimental condition. All data are expressed; the mean  $\pm$  the standard error of the mean (SEM). Statistical significance was evaluated by ANOVA followed by a Tukey's multiple comparison test.



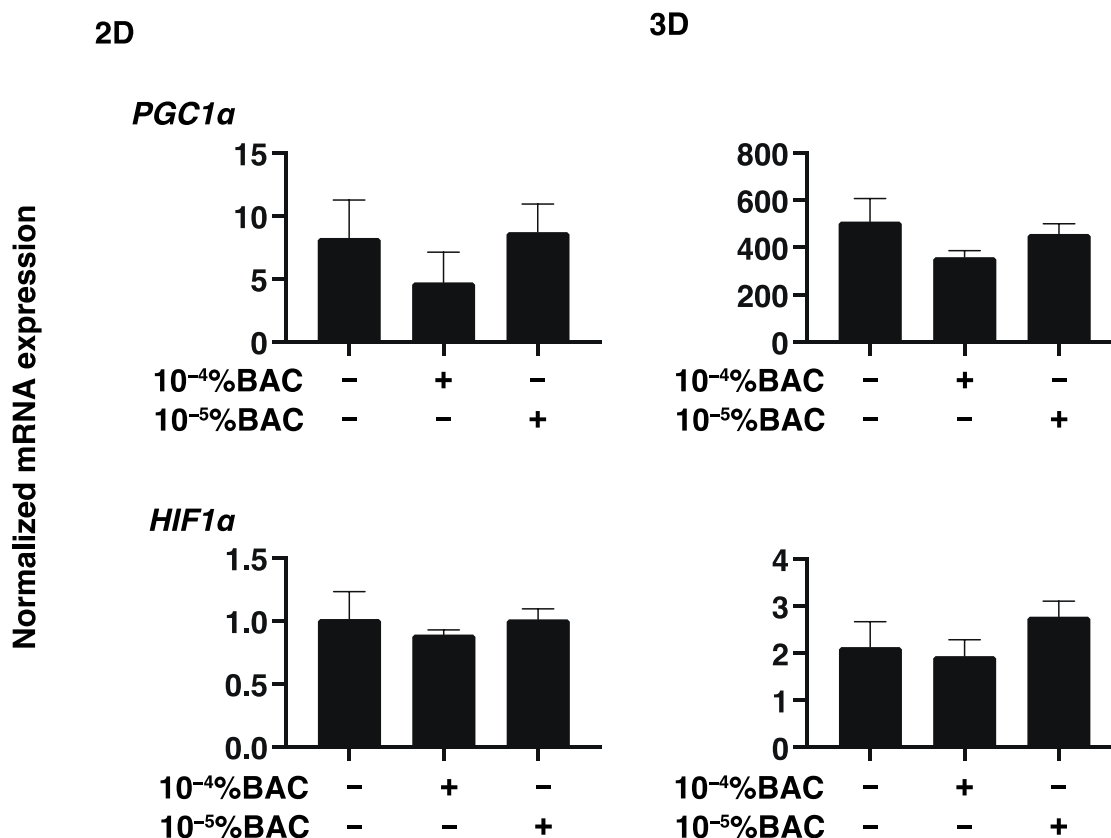


**Figure 6.** Effects of BAC on the gene expression of HIF1 and PGC1 $\alpha$  of HconF cells. 2D and 3D HconF cells were subjected to qPCR analysis in HIF1 $\alpha$  and PGC1 $\alpha$  and 14 in the absence or presence of 10<sup>-5</sup>% or 10<sup>-4</sup>% BAC. Experiments were repeated in triplicate using 3 different confluent 6-well dishes (2D) or 15 freshly prepared 3D HconF spheroids (3D) in each experimental condition. All data are expressed; the mean  $\pm$  the standard error of the mean (SEM). Statistical significance was evaluated by ANOVA followed by a Tukey's multiple comparison test.

#### 4. Discussion

Since BAC, a polyquaternary ammonium detergent, was registered as a safe additive by the Environmental Protection Agency (EPA) in the United States in 1947 due to its broad-spectrum antimicrobial properties, BAC is now widely used in numerous agricultural, industrial, and clinical products [45–47]. Alternatively, it has been pointed out that toxicities could be induced in humans and other animals by oral uptake, by inhalation, or via an epidermal (including the eye) route [48]. Although BAC has not been reported to be carcinogenic, mutagenic, or genotoxic, an in vitro study demonstrated that the BAC concentrations should be controlled to as low as 1 mg/L to avoid possible risks for BAC induced genotoxic effects within plant and mammalian cells [49]. Furthermore, considerable cell toxicity toward human ocular and intranasal cells were observed in vitro on exposure to BAC concentrations as low as 10<sup>-3</sup>% [50] and 45  $\times$  10<sup>-4</sup>% [51] respectively. In fact, the European Chemical Agency (ECHA) labels BAC as “causing severe skin burns and eye damage, is very toxic to aquatic life, is harmful if swallowed, and is harmful in contact with skin”. Therefore, extensive in vivo as well as in vitro studies must be conducted in the case of using drugs containing BAC, including instillations.

Biochemically, it is known that BAC is capable of lysing cell membranes [52] and thus break cell–cell junctions within the corneal epithelium resulting in facilitating the penetration of the topically applied drugs into the anterior chamber [52,53]. It has been reported that BAC in topical ophthalmic formulations can penetrate through the ocular surface into the anterior chamber as well as the optic nerve [54,55]. Alternatively, it is also well known that BAC induces a number of adverse effects by stimulating inflammation in ocular surface

tissues such as the conjunctiva [56–59]. In fact, a recent study reported that BAC exerts dose-dependent BAC toxic effects toward ocular surface epithelial cells using a mouse dry eye model [60]. Among several analyses using corneo-limbal epithelial cells (CLECs) in this study, a 24 h exposure of  $10^{-2}\%$  BAC resulted in a significantly increased cytotoxicity, as evidenced by LDH assays as well as flow cytometry data on AnnV/PI stained cells as compared with non-treated controls. More interestingly, a significant reduction in both the colony forming efficiency and the colony size of the CLEC cultures were observed when the exposure involved a  $10^{-4}\%$  BAC solution. Such BAC-induced effects at lower concentrations were also detected by the mitochondrial analysis of human corneal epithelial cells [61], that is, BAC inhibited ATP production (IC<sub>50</sub>, 5.3  $\mu\text{M}$ ;  $19 \times 10^{-5}\%$ ) and O<sub>2</sub> consumption (IC<sub>50</sub>, 10.9  $\mu\text{M}$ ;  $39 \times 10^{-4}\%$ ) and this inhibition was concentration-dependent. Taking the cationic property of BAC [52], a quaternary ammonium, into account, this observation is rationally supported by the fact that one of the major targets of BAC in the cell may be the only intracellular negatively charged mitochondria despite little information related to the influence of BAC on mitochondria.

Indeed, the findings presented in this study also demonstrated that significant reductions in mitochondrial and glycolytic reserve capacity are induced on exposure to BAC at concentrations of both  $10^{-5}\%$  and  $10^{-4}\%$  in 2D cultured HconF cells despite the fact that other analyses, including the barrier function of 2D monolayers, the physical properties of the 3D spheroids, and the mRNA expressions of several gene of ECM proteins, TIMPs, MMPs, and ER stress related factors were affected. Mitochondrial and glycolytic reserve refers to the ability of a cell to meet increased energy demands, and the retention of plasticity in these metabolic capacities has been reported to prevent cells from being driven into cellular senescence or cell death [62]. Therefore, the reduction of intracellular metabolic reserve induced by BAC exposure may potentially lead to an exacerbated cell dysfunction and cell death in HconF cells. However, as study limitations in the current investigation, additional information such as oxidative stress measurements, for instance, ROS production, or apoptosis will be required to confirm this speculation.

In conclusion, BAC, even at low concentrations, causes the deterioration of intracellular metabolic capacity in HconF cells. Since mitochondria play an indispensable role to maintain proper cellular functions, the effects of BAC noted herein raise great concerns for clinicians who are taking care of patients that are being administered formulations containing BAC, especially in cases of extended use.

**Supplementary Materials:** The following supporting information can be downloaded at: <https://www.mdpi.com/article/10.3390/biomedicines10092315/s1>, Figure S1: Cytotoxicity assay; Table S1: Sequences of primers used in qPCR.

**Author Contributions:** Author contributions: Y.T. performed the experiments, analyzed data, and wrote the paper. T.S. performed the experiments, analyzed data, and wrote the paper. M.W. performed experiments, analyzed data, and wrote the paper. M.F. analyzed the data. A.U. analyzed the data. Y.I. performed experiments. F.H. performed experiments. H.O. designed the experiments, analyzed the data, and wrote the manuscript. All authors have read and agreed to the published version of the manuscript.

**Funding:** This research received no external funding.

**Institutional Review Board Statement:** Not applicable.

**Informed Consent Statement:** Not applicable.

**Data Availability Statement:** The data that support the findings of this study are available from the corresponding author upon reasonable request.

**Conflicts of Interest:** The authors declare no conflict of interest.

## References

1. Leung, E.W.; Medeiros, F.A.; Weinreb, R.N. Prevalence of ocular surface disease in glaucoma patients. *J. Glaucoma* **2008**, *17*, 350–355. [[CrossRef](#)]
2. Fechtner, R.D.; Godfrey, D.G.; Budenz, D.; Stewart, J.A.; Stewart, W.C.; Jasek, M.C. Prevalence of ocular surface complaints in patients with glaucoma using topical intraocular pressure-lowering medications. *Cornea* **2010**, *29*, 618–621. [[CrossRef](#)]
3. Katz, G.; Springs, C.L.; Craven, E.R.; Montecchi-Palmer, M. Ocular surface disease in patients with glaucoma or ocular hypertension treated with either BAK-preserved latanoprost or BAK-free travoprost. *Clin. Ophthalmol.* **2010**, *4*, 1253–1261. [[CrossRef](#)] [[PubMed](#)]
4. Rossi, G.C.; Pasinetti, G.M.; Scudeller, L.; Raimondi, M.; Lanteri, S.; Bianchi, P.E. Risk factors to develop ocular surface disease in treated glaucoma or ocular hypertension patients. *Eur. J. Ophthalmol.* **2013**, *23*, 296–302. [[CrossRef](#)] [[PubMed](#)]
5. Baudouin, C.; Labbé, A.; Liang, H.; Pauly, A.; Brignole-Baudouin, F. Preservatives in eyedrops: The good, the bad and the ugly. *Prog. Retin. Eye Res.* **2010**, *29*, 312–334. [[CrossRef](#)] [[PubMed](#)]
6. Goldstein, M.H.; Silva, F.Q.; Blender, N.; Tran, T.; Vantipalli, S. Ocular benzalkonium chloride exposure: Problems and solutions. *Eye* **2022**, *36*, 361–368. [[CrossRef](#)] [[PubMed](#)]
7. Ammar, D.A.; Noecker, R.J.; Kahook, M.Y. Effects of benzalkonium chloride-preserved, polyquad-preserved, and sofZia-preserved topical glaucoma medications on human ocular epithelial cells. *Adv. Ther.* **2010**, *27*, 837–845. [[CrossRef](#)] [[PubMed](#)]
8. Ayaki, M.; Iwasawa, A. Cytotoxicity of prostaglandin analog eye drops preserved with benzalkonium chloride in multiple corneoconjunctival cell lines. *Clin. Ophthalmol.* **2010**, *4*, 919–924. [[CrossRef](#)]
9. Kim, J.H.; Kim, E.J.; Kim, Y.H.; Kim, Y.I.; Lee, S.H.; Jung, J.C.; Lee, K.W.; Park, Y.J. In vivo effects of preservative-free and preserved prostaglandin analogs: Mouse ocular surface study. *Korean J. Ophthalmol.* **2015**, *29*, 270–279. [[CrossRef](#)] [[PubMed](#)]
10. Pauly, A.; Brasnu, E.; Riancho, L.; Brignole-Baudouin, F.; Baudouin, C. Multiple endpoint analysis of BAC-preserved and unpreserved anti-allergic eye drops on a 3D-reconstituted corneal epithelial model. *Mol. Vis.* **2011**, *17*, 745–755.
11. Guzman-Aranguez, A.; Calvo, P.; Roperio, I.; Pintor, J. In vitro effects of preserved and unpreserved anti-allergic drugs on human corneal epithelial cells. *J. Ocul. Pharmacol. Ther.* **2014**, *30*, 790–798. [[CrossRef](#)] [[PubMed](#)]
12. Kim, Y.H.; Jung, J.C.; Jung, S.Y.; Yu, S.; Lee, K.W.; Park, Y.J. Comparison of the efficacy of fluorometholone with and without benzalkonium chloride in ocular surface disease. *Cornea* **2016**, *35*, 234–242. [[CrossRef](#)] [[PubMed](#)]
13. Liang, H.; Brignole-Baudouin, F.; Riancho, L.; Baudouin, C. Reduced in vivo ocular surface toxicity with polyquad-preserved travoprost versus benzalkonium-preserved travoprost or latanoprost ophthalmic solutions. *Ophthalmic Res.* **2012**, *48*, 89–101. [[CrossRef](#)] [[PubMed](#)]
14. Kahook, M.Y.; Noecker, R. Quantitative analysis of conjunctival goblet cells after chronic application of topical drops. *Adv. Ther.* **2008**, *25*, 743–751. [[CrossRef](#)] [[PubMed](#)]
15. Ammar, D.A.; Kahook, M.Y. Effects of glaucoma medications and preservatives on cultured human trabecular meshwork and non-pigmented ciliary epithelial cell lines. *Br. J. Ophthalmol.* **2011**, *95*, 1466–1469. [[CrossRef](#)]
16. Izzotti, A.; La Maestra, S.; Micale, R.T.; Longobardi, M.G.; Saccà, S.C. Genomic and post-genomic effects of anti-glaucoma drugs preservatives in trabecular meshwork. *Mutat. Res.* **2015**, *772*, 1–9. [[CrossRef](#)] [[PubMed](#)]
17. Kahook, M.Y.; Noecker, R.J. Comparison of corneal and conjunctival changes after dosing of travoprost preserved with sofZia, latanoprost with 0.02% benzalkonium chloride, and preservative-free artificial tears. *Cornea* **2008**, *27*, 339–343. [[CrossRef](#)] [[PubMed](#)]
18. Nagai, N.; Murao, T.; Okamoto, N.; Ito, Y. Comparison of corneal wound healing rates after instillation of commercially available latanoprost and travoprost in rat debrided corneal epithelium. *J. Oleo Sci.* **2010**, *59*, 135–141. [[CrossRef](#)] [[PubMed](#)]
19. Aihara, M.; Oshima, H.; Araie, M. Effects of SofZia-preserved travoprost and benzalkonium chloride-preserved latanoprost on the ocular surface—A multicentre randomized single-masked study. *Acta Ophthalmol.* **2013**, *91*, e7–e14. [[CrossRef](#)] [[PubMed](#)]
20. Aihara, M.; Ikeda, Y.; Mizoue, S.; Arakaki, Y.; Kita, N.; Kobayashi, S. Effect of switching to travoprost preserved with SofZia in glaucoma patients with chronic superficial punctate keratitis while receiving BAK-preserved latanoprost. *J. Glaucoma* **2016**, *25*, e610–e614. [[CrossRef](#)]
21. Horsley, M.B.; Kahook, M.Y. Effects of prostaglandin analog therapy on the ocular surface of glaucoma patients. *Clin. Ophthalmol.* **2009**, *3*, 291–295. [[CrossRef](#)] [[PubMed](#)]
22. García-Feijoo, J.; Muñoz-Negrete, F.J.; Hubatsch, D.A.; Rossi, G.C. Efficacy and tolerability of benzalkonium chloride-free travoprost in glaucoma patients switched from benzalkonium chloride-preserved latanoprost or bimatoprost. *Clin. Ophthalmol.* **2016**, *10*, 2085–2091. [[CrossRef](#)] [[PubMed](#)]
23. Lopes, J.F.; Hubatsch, D.A.; Amaris, P. Effect of benzalkonium chloride-free travoprost on intraocular pressure and ocular surface symptoms in patients with glaucoma previously on latanoprost: An open-label study. *BMC Ophthalmol.* **2015**, *15*, 166. [[CrossRef](#)] [[PubMed](#)]
24. Rossi, G.C.; Scudeller, L.; Rolle, T.; Pasinetti, G.M.; Bianchi, P.E. From benzalkonium chloride-preserved Latanoprost to Polyquad-preserved Travoprost: A 6-month study on ocular surface safety and tolerability. *Expert Opin. Drug Saf.* **2015**, *14*, 619–623. [[CrossRef](#)]
25. Ye, J.; Wu, H.; Zhang, H.; Wu, Y.; Yang, J.; Jin, X.; Shi, X. Role of benzalkonium chloride in DNA strand breaks in human corneal epithelial cells. *Graefes Arch. Clin. Exp. Ophthalmol.* **2011**, *249*, 1681–1687. [[CrossRef](#)] [[PubMed](#)]

26. Oouchi, Y.; Watanabe, M.; Ida, Y.; Ohguro, H.; Hikage, F. Rosiglitazone and ROCK inhibitors modulate fibrogenetic changes in TGF- $\beta$ 2 treated human conjunctival fibroblasts (HconF) in different manners. *Int. J. Mol. Sci.* **2021**, *22*, 7335. [[CrossRef](#)] [[PubMed](#)]
27. Kaneko, Y.; Ohta, M.; Inoue, T.; Mizuno, K.; Isobe, T.; Tanabe, S.; Tanihara, H. Effects of K-115 (Ripasudil), a novel ROCK inhibitor, on trabecular meshwork and Schlemm's canal endothelial cells. *Sci. Rep.* **2016**, *6*, 19640. [[CrossRef](#)]
28. Sato, T.; Chang, H.C.; Bayeva, M.; Shapiro, J.S.; Ramos-Alonso, L.; Kouzu, H.; Jiang, X.; Liu, T.; Yar, S.; Sawicki, K.T.; et al. mRNA-binding protein tristetraprolin is essential for cardiac response to iron deficiency by regulating mitochondrial function. *Proc. Natl. Acad. Sci. USA* **2018**, *115*, E6291–E6300. [[CrossRef](#)] [[PubMed](#)]
29. Sato, T.; Ichise, N.; Kobayashi, T.; Fusagawa, H.; Yamazaki, H.; Kudo, T.; Tohse, N. Enhanced glucose metabolism through activation of HIF-1 $\alpha$  covers the energy demand in a rat embryonic heart primordium after heartbeat initiation. *Sci. Rep.* **2022**, *12*, 74. [[CrossRef](#)] [[PubMed](#)]
30. Hikage, F.; Atkins, S.; Kahana, A.; Smith, T.J.; Chun, T.H. HIF2A-LOX Pathway promotes fibrotic tissue remodeling in thyroid-associated orbitopathy. *Endocrinology* **2019**, *160*, 20–35. [[CrossRef](#)]
31. Ota, C.; Ida, Y.; Ohguro, H.; Hikage, F. ROCK inhibitors beneficially alter the spatial configuration of TGF $\beta$ 2-treated 3D organoids from a human trabecular meshwork (HTM). *Sci. Rep.* **2020**, *10*, 20292. [[CrossRef](#)] [[PubMed](#)]
32. Ida, Y.; Hikage, F.; Itoh, K.; Ida, H.; Ohguro, H. Prostaglandin F2 $\alpha$  agonist-induced suppression of 3T3-L1 cell adipogenesis affects spatial formation of extra-cellular matrix. *Sci. Rep.* **2020**, *10*, 7958. [[CrossRef](#)] [[PubMed](#)]
33. Itoh, K.; Hikage, F.; Ida, Y.; Ohguro, H. Prostaglandin F2 $\alpha$  agonists negatively modulate the size of 3D organoids from primary human orbital fibroblasts. *Investig. Ophthalmol. Vis. Sci.* **2020**, *61*, 13. [[CrossRef](#)] [[PubMed](#)]
34. Ramos, T.; Scott, D.; Ahmad, S. An update on ocular surface epithelial stem cells: Cornea and conjunctiva. *Stem Cells Int.* **2015**, *2015*, 601731. [[CrossRef](#)]
35. Nadri, S.; Soleimani, M.; Kiani, J.; Atashi, A.; Izadpanah, R. Multipotent mesenchymal stem cells from adult human eye conjunctiva stromal cells. *Differentiation* **2008**, *76*, 223–231. [[CrossRef](#)]
36. Lee, M.J.; Ko, A.Y.; Ko, J.H.; Lee, H.J.; Kim, M.K.; Wee, W.R.; Khwarg, S.I.; Oh, J.Y. Mesenchymal stem/stromal cells protect the ocular surface by suppressing inflammation in an experimental dry eye. *Mol. Ther. J. Am. Soc. Gene Ther.* **2015**, *23*, 139–146. [[CrossRef](#)] [[PubMed](#)]
37. Bouchemi, M.; Roubex, C.; Kessal, K.; Riancho, L.; Raveu, A.L.; Soualmia, H.; Baudouin, C.; Brignole-Baudouin, F. Effect of benzalkonium chloride on trabecular meshwork cells in a new in vitro 3D trabecular meshwork model for glaucoma. *Toxicol. Vitr.* **2017**, *41*, 21–29. [[CrossRef](#)] [[PubMed](#)]
38. Khoh-Reiter, S.; Jessen, B.A. Evaluation of the cytotoxic effects of ophthalmic solutions containing benzalkonium chloride on corneal epithelium using an organotypic 3-D model. *BMC Ophthalmol.* **2009**, *9*, 5. [[CrossRef](#)]
39. Watanabe, M.; Ida, Y.; Ohguro, H.; Ota, C.; Hikage, F. Establishment of appropriate glaucoma models using dexamethasone or TGF $\beta$ 2 treated three-dimension (3D) cultured human trabecular meshwork (HTM) cells. *Sci. Rep.* **2021**, *11*, 19369. [[CrossRef](#)]
40. Ida, Y.; Umetsu, A.; Furuhashi, M.; Watanabe, M.; Tsugeno, Y.; Suzuki, S.; Hikage, F.; Ohguro, H. ROCK 1 and 2 affect the spatial architecture of 3D spheroids derived from human corneal stromal fibroblasts in different manners. *Sci. Rep.* **2022**, *12*, 7419. [[CrossRef](#)] [[PubMed](#)]
41. Hikage, F.; Ichioka, H.; Watanabe, M.; Umetsu, A.; Ohguro, H.; Ida, Y. ROCK inhibitors modulate the physical properties and adipogenesis of 3D spheroids of human orbital fibroblasts in different manners. *FASEB BioAdvances* **2021**, *3*, 866–872. [[CrossRef](#)] [[PubMed](#)]
42. Hikage, F.; Ida, Y.; Ouchi, Y.; Watanabe, M.; Ohguro, H. Omidenepag, a selective, prostanoid EP2 agonist, does not suppress adipogenesis in 3D organoids of human orbital fibroblasts. *Transl. Vis. Sci. Technol.* **2021**, *10*, 6. [[CrossRef](#)]
43. Rogov, A.G.; Goleva, T.N.; Sukhanova, E.I.; Epremyan, K.K.; Trendeleva, T.A.; Ovchenkova, A.P.; Aliverdieva, D.A.; Zvyagilskaya, R.A. Mitochondrial dysfunctions may be one of the major causative factors underlying detrimental effects of benzalkonium chloride. *Oxidative Med. Cell. Longev.* **2020**, *2020*, 8956504. [[CrossRef](#)]
44. Battaglia, F.; Scambia, G.; Distefano, M.; Ronca, S.; Plotti, F.; Plotti, G.; Mancuso, S. Quaternary ammonium salts in gynecology and obstetrics. *Minerva Ginecol.* **2000**, *52*, 471–484. [[PubMed](#)]
45. Merchel Piovesan Pereira, B.; Tagkopoulos, I. Benzalkonium chlorides: Uses, regulatory status, and microbial resistance. *Appl. Environ. Microbiol.* **2019**, *85*, e00377-19. [[CrossRef](#)] [[PubMed](#)]
46. Choi, S.M.; Roh, T.H.; Lim, D.S.; Kacew, S.; Kim, H.S.; Lee, B.M. Risk assessment of benzalkonium chloride in cosmetic products. *J. Toxicol. Environ. Health Part B Crit. Rev.* **2018**, *21*, 8–23. [[CrossRef](#)] [[PubMed](#)]
47. Condell, O.; Iversen, C.; Cooney, S.; Power, K.A.; Walsh, C.; Burgess, C.; Fanning, S. Efficacy of biocides used in the modern food industry to control salmonella enterica, and links between biocide tolerance and resistance to clinically relevant antimicrobial compounds. *Appl. Environ. Microbiol.* **2012**, *78*, 3087–3097. [[CrossRef](#)] [[PubMed](#)]
48. Basketter, D.A.; Marriott, M.; Gilmour, N.J.; White, I.R. Strong irritants masquerading as skin allergens: The case of benzalkonium chloride. *Contact Dermat.* **2004**, *50*, 213–217. [[CrossRef](#)]
49. Ferik, F.; Misik, M.; Hoelzl, C.; Uhl, M.; Fuerhacker, M.; Grillitsch, B.; Parzefall, W.; Nersesyan, A.; Micieta, K.; Grummt, T.; et al. Benzalkonium chloride (BAC) and dimethyldioctadecyl-ammonium bromide (DDAB), two common quaternary ammonium compounds, cause genotoxic effects in mammalian and plant cells at environmentally relevant concentrations. *Mutagenesis* **2007**, *22*, 363–370. [[CrossRef](#)]

50. De Saint Jean, M.; Brignole, F.; Bringuier, A.F.; Bauchet, A.; Feldmann, G.; Baudouin, C. Effects of benzalkonium chloride on growth and survival of Chang conjunctival cells. *Investig. Ophthalmol. Vis. Sci.* **1999**, *40*, 619–630.
51. Marple, B.; Roland, P.; Benninger, M. Safety review of benzalkonium chloride used as a preservative in intranasal solutions: An overview of conflicting data and opinions. *Otolaryngol. Head Neck Surg.* **2004**, *130*, 131–141. [[CrossRef](#)] [[PubMed](#)]
52. Tripathi, B.J.; Tripathi, R.C.; Kolli, S.P. Cytotoxicity of ophthalmic preservatives on human corneal epithelium. *Lens Eye Toxic. Res.* **1992**, *9*, 361–375.
53. Yee, R.W. The effect of drop vehicle on the efficacy and side effects of topical glaucoma therapy: A review. *Curr. Opin. Ophthalmol.* **2007**, *18*, 134–139. [[CrossRef](#)] [[PubMed](#)]
54. Brignole-Baudouin, F.; Desbenoit, N.; Hamm, G.; Liang, H.; Both, J.P.; Brunelle, A.; Fournier, I.; Guerineau, V.; Legouffe, R.; Stauber, J.; et al. A new safety concern for glaucoma treatment demonstrated by mass spectrometry imaging of benzalkonium chloride distribution in the eye, an experimental study in rabbits. *PLoS ONE* **2012**, *7*, e50180. [[CrossRef](#)]
55. Stevens, A.M.; Kestelyn, P.A.; De Bacquer, D.; Kestelyn, P.G. Benzalkonium chloride induces anterior chamber inflammation in previously untreated patients with ocular hypertension as measured by flare meter: A randomized clinical trial. *Acta Ophthalmol.* **2012**, *90*, e221–e224. [[CrossRef](#)] [[PubMed](#)]
56. Malvitte, L.; Montange, T.; Vejux, A.; Baudouin, C.; Bron, A.M.; Creuzot-Garcher, C.; Lizard, G. Measurement of inflammatory cytokines by multicytokine assay in tears of patients with glaucoma topically treated with chronic drugs. *Br. J. Ophthalmol.* **2007**, *91*, 29–32. [[CrossRef](#)]
57. Sherwood, M.B.; Grierson, I.; Millar, L.; Hitchings, R.A. Long-term morphologic effects of antiglaucoma drugs on the conjunctiva and Tenon's capsule in glaucomatous patients. *Ophthalmology* **1989**, *96*, 327–335. [[CrossRef](#)]
58. Lavin, M.J.; Wormald, R.P.; Migdal, C.S.; Hitchings, R.A. The influence of prior therapy on the success of trabeculectomy. *Arch. Ophthalmol.* **1990**, *108*, 1543–1548. [[CrossRef](#)]
59. Broadway, D.C.; Grierson, I.; O'Brien, C.; Hitchings, R.A. Adverse effects of topical antiglaucoma medication. II. The outcome of filtration surgery. *Arch. Ophthalmol.* **1994**, *112*, 1446–1454. [[CrossRef](#)]
60. Zhang, R.; Park, M.; Richardson, A.; Tedla, N.; Pandzic, E.; de Paiva, C.S.; Watson, S.; Wakefield, D.; Di Girolamo, N. Dose-dependent benzalkonium chloride toxicity imparts ocular surface epithelial changes with features of dry eye disease. *Ocul. Surf.* **2020**, *18*, 158–169. [[CrossRef](#)]
61. Datta, S.; Baudouin, C.; Brignole-Baudouin, F.; Denoyer, A.; Cortopassi, G.A. The eye drop preservative benzalkonium chloride potently induces mitochondrial dysfunction and preferentially affects LHON mutant cells. *Investig. Ophthalmol. Vis. Sci.* **2017**, *58*, 2406–2412. [[CrossRef](#)] [[PubMed](#)]
62. Desler, C.; Hansen, T.L.; Frederiksen, J.B.; Marcker, M.L.; Singh, K.K.; Rasmussen, L.J. Is there a link between mitochondrial reserve respiratory capacity and aging? *J. Aging Res.* **2012**, *2012*, 192503. [[CrossRef](#)] [[PubMed](#)]